NASA Contractor Report 165984

AUTOMATED DESIGN OF MINIMUM DRAG LIGHT AIRCRAFT FUSELAGES AND NACELLES

Frederick O. Smetana, Stan R. Fox, and
Baruch E. Karlin

NORTH CAROLINA STATE UNIVERSITY
Raleigh, North Carolina 27607

Grant NSG-1584
September 1982

National Aeronautics and
Space Administration

Langley Research Center
Hampton, Virginia 23665

Automated Design of Minimum Drag Light Aircraft Fuselages and Nacelles

by

Frederick O. Smetana
Stan R. Fox
Baruch E. Karlin

Department of Mechanical and Aerospace Engineering
North Carolina State University, Raleigh, NC

Abstract

The constrained minimization algorithm of Vanderplaats is applied to the problem of designing minimum drag faired bodies such as fuselages and nacelles. Body drag is computed by a variation of the Hess-Smith code. This variation includes a boundary layer computation. The encased payload provides arbitrary geometric constraints--specified a priori by the designer--below which the fairing cannot shrink. The optimization may include engine cooling air flows entering and exhausting through specific port locations on the body.

Introduction

Despite many protestations to the contrary, flight vehicle design has always been more art than science. It has, of course, been possible for some time to design simple shapes like projectiles according to formulae which can be shown to yield minimum wave drag for a given maximum cross section and volume; but, for more complex shapes the process has always involved considerable cut and try as well as design experience and aesthetics.

However, this situation may soon change as the result of the confluence of three factors: (1) the development of practical algorithms to minimize objective functions which are subject to a variety of physical constraints; (2) the development of flow analysis techniques which can provide accurate results even for complex bodies at the end of which there is a small amount of flow separation; and (3) the arrival of computers with sufficient speed and memory capacity to run such codes efficiently and at reasonable cost. Before long it should be possible to routinely encase almost any size and shape payload in a minimum drag fairing specifically designed for that payload. It will also be possible to include in the optimization consideration items such as fairing weight, flow quantity into and out of the fairing, and the location on the body of the inlet and exhaust flow ports.

There are two very powerful economic incentives for following such an approach: (1) except for a small amount needed to increase the vehicle's energy, all of an aircraft's fuel is burned overcoming drag and (2) a cut and try approach to aircraft drag minimization is extremely costly in time, in engineering and technician labor, and even to some extent in wasted materials.

It has long been recognized that the drag increment due to the installation of an air-cooled piston engine is related in some fashion to its cross sectional area. It has, therefore, been the practice to cowl it as tightly as possible while leaving adequate room for accessories, ducting, and cooling air flow. Within these constraints it is usually left to the designer's eye to determine the exact cowl shape. Only if the resulting aircraft's performance is far below predictions would one normally expect to examine the adequacy of the nacelle or forward fuselage design by way of test program perhaps combined with an extensive analytical investigation.

It is also known that the drag associated with the flow of cooling air through nacelle inlets, engine fins and baffles, and nacelle exhausts can represent as much as 25% of the total vehicle drag.[1] This figure, even without considering the drag increment due to an improperly-shaped cowl, is sufficiently large to justify serious attempts at developing a rigorous design technique guaranteed to produce a minimum-drag, nacelle-flow combination.

An analytical optimization technique is desired which can indicate how the body shape should be modified so as to yield a demonstrable minimum drag. Obviously, this must be coupled to a sufficiently accurate fluid dynamic model of the vehicle so that the measured drag resulting from these shape changes will in fact be very close to the drag calculated. This is a report on a NASA-supported research project at North Carolina State University which has this objective as its goal.

The Optimizer

The function to be minimized is the steady-state drag of a fairing about a specific "payload." Payload is here taken to mean such things as an engine, a passenger compartment, etc. The payload provides specific geometric constraints limiting the minimum fairing size.

The payload is not necessarily regular or symmetric about any axis. A variety of optimizers could be used. It has, however, been the experience of many workers in the optimization field that the best

method to use in a specific situation often depends upon the problem at hand and cannot readily be foretold. Those who have worked in the field for some time are also aware of the difficulty of developing new codes--even those following established procedures--from scratch. The use of generally available optimization codes whenever possible is therefore highly desirable. One of the most versatile of these is that developed over the past ten years or so by Garrett N. Vanderplaats[2] of the NASA Ames Laboratory and the Naval Postgraduate School. Further, it has been applied successfully to a number of related optimization problems (airfoil design).[3] This code employs the method of feasible directions.

The Vanderplaats procedure has been formulated as a numerical optimization problem which may be stated as follows:

$$\text{minimize} \quad OBJ = F(\bar{X})$$

$$\text{subject to} \quad G_i(\bar{X}) \leq p \quad (i = 1,m)$$

$$X_i^{\ell} \leq X_i \leq X_i^{u} \quad (i = 1,n)$$

In the present case, the objective function is the body drag. The vector $\bar{X}$ contains n design variables. For axisymmetric bodies we have chosen n = 5. For more general bodies with a plane of symmetry represented by a set of 14 panels over the half body, we take n = 15 * 5 = 75 The vector $\bar{X}$ contains the amplitudes of the shape functions ($0 \leq x \leq 1$)

$$F_1 = x^{0.25} * (1 - x)/e^{20x}$$

$$F_2 = \sin(\pi x^{0.431})^3$$

$$F_3 = \sin(\pi x^{0.757})^3$$

$$F_4 = \sin(\pi x^{1.357})^3$$

$$F_5 = \sin(\pi x^{3.106})^3$$

(Here x refers to the non-dimensional distance from the body nose.)

which are employed to change the shape of the body locally along a line reaching from the nose to the tail.* For the axisymmetric body, every circumferential panel is given the same modification when one shape

---

*The exponents on x determine the axial station at which that function produces its maximum influence on the body shape. These exponent values may be problem dependent.

function amplitude is varied. For the general body, the surface shape modifications due to a change in one shape function amplitude are applied along a line of panel boundaries reaching from nose to tail. The shape function amplitudes in $\bar{X}$ are to be changed in such a way that drag is minimized satisfying the constraints. $G_j(\bar{X})$ defines the constraints which the designer wishes to impose on the optimization problem. $F(\bar{X})$ and $G_j(\bar{X})$ may be either implicit or explicit functions of the design variables $\bar{X}$ but must be continuous. In the present problem, $F(\bar{X})$ is implicit but $G_j(\bar{X})$ is explicit, representing the *m* major physical dimensions of the inscribed payload.

Variables $\bar{X}_i^{\ell}$ and $\bar{X}_i^{u}$ define the lower and upper bounds, respectively, on the design variables and are the limits over which $F(\bar{X})$ and $G_j(\bar{X})$ are defined. For the problem being considered $\bar{X}_i^{u}$ is unbounded. If the inequality condition $G_j(\bar{X}) > 0$ is violated for any constraint, the constraint is said to be violated. If the equality condition G_j $G_j(\bar{X}) = 0$ is met, the constraint is called active and if the strict inequality condition $G_j(\bar{X}) < 0$ is met, the constraint is inactive. Computationally an exact zero can seldom be achieved; thus a constraint is called active if its value is within a specified tolerance of zero.

The n-dimensional space spanned by the design variables $\bar{X}$ is referred to as the design space. Any design which satisfies the inequality equations is referred to as a feasible design. If the design violates one or more of these inequalities, it is said to be infeasible. The minimum feasible design is said to be optimal.

The optimization program begins with an initial $\bar{X}$ vector which is input to the program and may or may not define a feasible design. (In the present case, we always begin with a circumscribing body larger than the minimum drag body and therefore always feasible design.) The optimization process then proceeds iteratively by the following recursive relationship:

$$\bar{X}^{q+1} = \bar{X}^{q} + \alpha^* \bar{S}^{q}$$

where q is the iteration number, vector $\bar{S}$ is the direction of search in the n-dimension design space, and α^* is a scalar which defines distance of travel and direction $\bar{S}$. The notation α^* for the move parameter is used here for consistency with mathematical programming nomenclature and should not be confused with the body angle of attack which, for reasons indicated below, is always zero.

The optimization process then proceeds in two steps. The first is the determination of a direction $\bar{S}$ which will reduce the objective function without violating the constraints. The second is the determination of a scalar α^* so that the objective function is minimized in this direction, a new constraint is encountered, or a currently active constraint is encountered again. For example, suppose an initial

design is given for which no constraints are active or violated. The program then begins by perturbing each of the $\bar{X}$ variables to determine its effect on the objective function (body drag, in this case). The gradient of C_D is calculated by finite difference using a single forward step and the gradient vector is constructed as

$$\bar{\nabla}OBJ = \begin{Bmatrix} \frac{\partial C_D}{\partial X_1} \\ \cdot \\ \cdot \\ \cdot \\ \frac{\partial C_D}{\partial X_N} \end{Bmatrix}$$

Because no constraints are active or violated, it is obvious that the greatest improvement in the objective function is obtained by moving in the negative gradient or steepest descent direction so that $\bar{S} = -\bar{\nabla}C_D$.

Having determined $\bar{S}$, the scalar α^* must now be determined so that either the objective function is minimized in this direction or some constraint boundary is encountered. That is, one-dimensional search is done in direction $\bar{S}$ to determine the appropriate value for α^* so that an improved design is obtained. No further improvement can be achieved in this direction; it is now necessary to determine a new $\bar{S}$ vector which will improve the design.

The second design iteration begins by again perturbing the design variables to obtain the gradient of the objective function, C_D. Now, instead of moving in a steepest descent direction, the $\bar{S}$ vector is calculated from the following relationship

$$\bar{S}^q = -\bar{\nabla}OBJ^q + \frac{\left|\bar{\nabla}OBJ^q\right|^2}{\left|\bar{\nabla}OBJ^{q-1}\right|^2}\bar{S}^{q-1}$$

This equation defines the conjugate direction as developed by Fletcher and Reeves. The advantage that this definition of the $\bar{S}$ vector has over the steepest descent direction is that if the objective is a quadratic function of the design variables, covergence to the optimum can be guaranteed to occur in n iterations or less. Although most problems of practical interest are not quadratic functions of the design variables, they may still be approximated as quadratic in the region of the solution. In other words, if the first three terms of a Taylor series expansion of the objective function form a reasonable

approximation to that function, then the foregoing equation can be expected to provide more rapid convergence than a steepest descent search, since steepest descent uses only the first two terms of the Taylor series expansion. Having determined the new direction $\overline{S}$, one searches in that direction until another constraint is encountered, which ends the second design iteration.

The design variables are again perturbed to obtain the gradient of the objective function, C_D. At the same time, the gradient of the active constraint is obtained. Now a search direction must be found which will reduce the objective function without violating the active constraint. Such a direction can be found by solving the following subproblem which is a linear programming problem with a single quadratic constraint.

Find $\overline{S}$ to maximize β

Subject to:

$$\overline{\nabla OBJ}(\overline{X}) \cdot \overline{S} + \beta \leq 0$$

$$\nabla G_u(\overline{X}) \cdot \overline{S} + \theta_j \beta \leq 0 \quad (j = 1,NAC)$$

$$\overline{S} \cdot \overline{S} \leq 1$$

NAC is the number of active constraints. The details for solving this problem are given by Zoutendijk[4] and by Vanderplaats and Moses.[5] Note that if the first equation is satisfied and β is positive, the resulting direction will reduce the objective function and is defined as a "usable" direction. If the second equation is satisfied and β is positive, $\overline{S}$ is called a feasible direction because, for a small move in this direction, no constraints will be violated. The prespecified parameter θ_j is referred to as a pushoff factor for the jth constraint and has the effect of pushing and design away from the active constraint. The value of θ_j must be zero or positive to maintain a feasible design. If θ_j were zero, the resulting direction would be precisely tangent to the active constraint. On the other hand, a very large θ_j would push the design away from the active constraint and nearly tangent to a line of constant objective function. A value of $\theta_j = 1$ will yield a direction which approximately bisects the angle between constant objective function and the constraint. If the maximum value of β obtainable from the above equations is zero, then no direction exists which will both reduce the objective function and satisfy the constraint. The current design is optimal or at least a local minimum.

As the number of design variables increase and the nonlinearity of the objective function increases, it will be necessary in practice to limit the size of α^* to prevent the body from becoming so distorted that that fluid dynamic analysis is not possible. Increasing the number of design variables and the nonlinearity of the objective function also increases the accuracy requirements on the fluid dynamic calculations since each design variable now contributes a smaller amount to the total gradient value and the contributions from different variables may range from nearly insignificant to very significant, a situation that may change from iteration to iteration as the body shape changes. Even without these accuracy requirements and move limitations, the computational time required increases approximately as the number of design variables squared. Thus, while a two-dimensional airfoil optimization problem involving 5 design variables may require perhaps two minutes per iteration and no more than 20 iterations to reach an optimum that also satisfies the constraints, the minimum drag body problem involving 75 design variables requires on the order of an hour per iteration and--depending upon the extent to which the optimization is carried out, e.g., whether the optimum is actually reached or merely closely approached--many more than 20 iterations.

The use of such mathematical techniques in design then becomes a question of economic trade-offs. The speed of digital processing is increasing and its relative cost is decreasing. Manual design labor, operation of test facilities for evaluating the effectiveness of body recontouring, and the energy cost of operating a body with more than optimal drag are all increasing. Thus it seems likely that if a mathematical analysis and optimization technique can be shown to yield accurate results, it will replace the traditional design and development technique in the near future.

Flow Analysis Model

In order to be useful in real situations, the flow model upon which the optimizer operates must be capable of accurately representing the flow over rather complex bodies. The authors had been involved in the development of such a code during the previous six years so it was natural for them to consider that code as the basis of the flow model for the present work. As is usually the case in such matters the code has a long pedigree. It began in 1962 as the work of John Hess and A. M. O. Smith[6] of the Douglas Aircraft Company in Long Beach, California. They chose to represent the potential flow over a body with a plane of symmetry through the following device: the surface of the body is represented by many plane quadrilaterals. (In the limit this representation becomes exact.) At the center of each panel is a

fluid source of undetermined strength. (One could also use a distributed source of constant strength over a panel.) The source strengths are determined by requiring that the flow induced by all sources interacting with the oncoming stream be parallel with the surface at one point on each panel.*

Charles W. Dawson and Janet Dean[7] of the Naval Ship Research and Development Center added to the Hess-Smith code the capability for calculating on-body and off-body streamlines in the early 1970's. At North Carolina State University we used this capability to do two-dimensional momentum integral boundary layer calculations along streamlines.[8] As a result, we were able to determine the skin friction at the center of each panel and the boundary layer displacement thickness in the aft regions of the body. Based on rather detailed surface pressure measurements on the Airship Akron which we found in the literature, we chose to assume that the flow separated from the body at a point two sets of panels forward from the rear of the body with an angle relative to the surface proportional to $d\delta^*/dx$. We then located the downstream stagnation point in such a way that the departing streamline would gradually fair to it, about one body diameter aft of the physical body. For calculating the pressure distribution on the body we assumed that the physical stern end of the body was replaced by this faired "wake body" and the pressures calculated for the first two sets of panels on the wake body were those applied to the last two sets of panels on the physical body. As a result, the real body evidences both a skin friction drag and a pressure drag.

It will be recognized that this device for obtaining body drag within the framework of a potential flow calculation rests on a number of rather arbitrary assumptions:

1. That the boundary layer flow can be analyzed as being two-dimensional along streamlines. This is approximately correct only when we are dealing with a relatively slender body at zero angle of attack. The method obviously fails in situations with large circumferential pressure gradients.

---

*Inlets and exhausts are represented by relaxing the requirement that the flow velocity normal to every panel surface be zero. This requirement is replaced by one specifying the direction and magnitude of the flow velocity normal to the surfaces of these panels which form inlets or exhausts the zero normal velocity requirement is retained for all other panels.

2. That a standard momentum-integral technique may be used. Momentum integral techniques have been shown to be reasonably accurate for constant velocity and accelerating flows. They do not give an accurate indication of the point of flow separation and yield too large a boundary layer in regions of decelerating flow--hence, the necessity of specifying the separation point (point for attachment of the wake body) rather arbitrarily. For this reason also, they give poor results for bodies with concave regions. (The potential flow method also has trouble with such regions.) Finite difference calculation of the boundary layer characteristics were rejected because of the very large computing time penalty involved and the present uncertain state of general three-dimensional boundary layer theory.

3. That the point of attachment and shape of the wake body can be specified a priori based on a limited correlation of body shape and drag.

Despite these arbitrary assumptions, calculated drag values were acceptably close to experimental values (less than 5% error) for those fuselages and nacelles for which we could find experimental results.

The version of the NCSU BODY code used for the present work does not include the panel normal velocity specification provision developed previously[9] which permits the representation of flow inlets and exhaust by specifying the entering and leaving flow velocities based on the external pressures and the internal flow restrictions. It also does not include a provision, supplied in an earlier version[10], for imposing the axial component of propeller slipstreams on the flow over the body. These provisions were omitted for the present in order to hold down the cost of runs during code development. One other cost-saving change of a rather fundamental nature was to eliminate most of the disk read-writes present in previous versions. This step resulted in a 40% improvement in execution time and a 30% reduction in cost. It also renders the code too large to execute on most computers without virtual memory capabilities.

Note, too, that the version of the potential flow code used here does not include some of the later provisions added by Hess and Smith such as the use of linear source distributions on curved panels. These provisions improve the accuracy of the code significantly for a modest increase in computer time.

Mating the Optimizer to the Flow Analyzer

In order to determine how the body shape must be altered to reduce the drag, the optimizer must evaluate a gradient (Δ drag/Δ shape) numerically. This gradient is a vector which contains an element representing the contribution from each variable specifying the body surface. If one were to use the corner coordinates of each panel as design variables one would have to go through the body flow analysis program N times, where N is the number of panels used to represent a half-body. When N is 600 or more, as it needs to be to adequately represent even moderately complex bodies, the computer time required becomes impractical even in this day of high speed computers. For this reason the use of shaping functions or reduced coordinates appears very attractive. These alter the body shape with fewer design variables. Each function alters a small region of the body surface rather than just a group of four panels. Some flexibility is sacrificed but by judicious choice of the shaping functions virtually any modification felicitous for drag reduction can be implemented. For our work, we choose to employ the same shape functions Haney and Johnson[11] used for their airfoil optimization work. Using this approach, we employ a group of five shape functions to represent the entire length of the body at each circumferential panel boundary. In other words, if one has a body represented by N axial panel boundaries and M circumferential panel boundaries for a total of (N-1)*(M-1) panels one can, through the use of these reduced coordinates (shape function amplitudes), reduce the number of design variables from N*M to 5*M.

This, then, was the plan of attack. As with many other plans, difficulties not anticipated in the conception phase arose during execution. The computation of the gradient involves taking differences between the drag of the unaltered body and that of the body with one design variable altered. Since the difference between the two values usually occurs in the third and fourth significant digits, an error of 5% in the drag computation is obviously not acceptable. This problem is evidenced by a rapidly varying sign on the gradient from iteration to iteration. Modifying the flow analyzer to execute in double precision seemed to resolve that problem.

It was noted earlier that the wake body was attached to the physical body two set of panels forward of the end of the physical body. While this arbitrary attachment point proved satisfactory for relatively streamlined bodies, the optimization scheme tended to squeeze the fore and aft ends of the physical body, leading to very steep pressure gradients toward the rear of the body. The computed drag would certainly decline as a result of such squeezing but in reality the flow cannot negotiate the large pressure rises indicated by the

computations in the vicinity of the rear end of the body. The obvious remedy is to move the wake body attachment point upstream to the point where the flow would normally separate under these circumstances and extend the downstream tip of the wake body (the stagnation point required by potential theory) further into the physical wake so that the rate of pressure rise with streamwise distance on the physical body is more realistic. Determination of when it is time to perform this action can be made in a number of ways. As discussed in the next section, the approach used in formulating the present code is to test $d\ell/dx$ all along the aft portion of the body-wake combination. If this value ever exceeds a trigger value, it is assumed that separation would have taken place. The wake attachment point is then moved upstream and the stagnation point downstream and the pressures are recomputed. The resulting wake bodies tend to become very long, shallow-angle cones, particularly if the attachment point had to be moved more than once to obtain an acceptable pressure distribution.

The existence of a large, gradually-tapered wake body can easily illuminate the existence of another problem. An integration of the pressures over the body cum wake body should yield, according to D'Alembert's principal, zero drag. However, the pressures are known only at the centroids of N flat panels representing the body surface. It is natural that one should carry out the force determination by assuming these pressures to exist over the entire panel and multiply the product of pressure and panel area by the cosine of the angle between the panel normal and the streamwise direction and then summing over all panels. For a long, thin wake body the pressure at the last panel's centroid, for example, is quite different from that at the downstream stagnation point. For an elliptical body represented by 400 panels errors as high as 35% can arise from this source. It is not practical to increase the number of panels used in the computation significantly since storage increases directly with N and the computational time per iteration increases as N^2 while the error is only one-half for twice as many panels. It is, therefore, necessary to attempt to fair the pressure distribution smoothly over the body and to integrate the variable pressure over each panel. This is a rather formidable task which seems to be best accomplished by transforming the panel to a square and employing a standard bi-cubic spline routine* to accomplish the pressure fairing and force integration.

---

*From the IMSL package.

Results and Discussion

Because of the shorter run times required, much of the development work with the code used the axisymmetric body option. The constraint body was a 3-to-1 ellipsoid and the circumscribing body a 2-to-1 ellipsoid. Figure 1 shows the circumscribing body. Figure 2 shows the body with the wake body attached over the last two sets of panels on the physical body. The drag coefficient which this arrangement yields is indicated beside the body.* The value reported in Rouse[12] for a 2-to-1 ellipsoid with turbulent boundary layer using the present normalization is 0.0127-0.01459. The body and wake configuration which the optimizer yields if one does not permit the separation point to move is shown in Figure 3. Figure 4 shows the wake and body combination obtained by allowing the separation point to move upstream in response to an excessive pressure rise near the aft end. This figure illustrates particularly well why the pressure at the center of the last set of panels--if assumed to exist over the entire panel--will integrate to a non-zero drag and why it is necessary to employ a variable pressure-area relationship, at least in this region, for accurate drag determination.

Since the wake is the crucial factor in determining the drag (the skin friction is only about 20% of the total drag of the original circumscribing body and does not change significantly with small variations in body configuration) the wake will also be the critical factor in determining whether and how fast the body diameter decreases to meet the constraint body. If the optimizer can shrink the wake alone it has little incentive to reduce the diameter of the circumscribing body. Thus, it is important that the gradient of the objective function be capable of including the effects of moving the separation point upstream and that a realistic criterion for the initiation of this movement be included in the routine.

At present, the routine calculates the change in pressure from panel centroid to panel centroid and divides this by the axial distance between centroids. Whenever this pressure gradient exceeds a present value (selected arbitrarily at this time by the user) it restarts the

---

*Note that one can make this number almost anything one desires by altering the location of the downstream stagnation point and the way the the "wake" is faired to the body. A downstream stagnation point located one body diameter aft of the stern combined with a wake having a rapid initial taper (so that the wake looks rather like a golf tee) will yield a low C_D value. On the other hand, if the downstream stagnation point is located, say, 10 body diameters downstream and the wake has almost no taper, C_D will be rather large. A 3-to-1 ellipsoid with a cylindrical wake attached at the maximum thickness station would yield a C_D of about 0.08 with the present method of normalization.

program with the wake attached two axial stations upstream. The pressure gradients are recomputed and if they again violate the preset limit, the wake attachment point is again moved upstream two more axial stations. The process is repeated until the pressure gradient on the body plus wake is everywhere below the preset value or the wake is attached at the axial station corresponding to the maximum body diameter or at the first station downstream of the maximum body diameter. Because the pressures on the aft end of the physical body are then quite low, the optimizer will shrink the body rapidly as shown in Figure 5.

If the "pushoff factor" is set too small, the body produced by the optimizer will violate the constraints. See Figure 6. On the other hand, making the constraints too elastic (pushoff factor too large) results in the generation of a large disc-like body with a rapidly tapering wake once the constraints are encountered. This type of wake occurs because of the necessity of specifying the downstream extent of the wake a priori in terms of the original body diameter. For this reason the wake contours become very unrealistic if the diameter of the body produced by the optimizer is greatly increased. Figures 7 and 8 depict this rather forcefully.

In operating the program one must also learn to adjust the relative strengths of the shaping functions and the axial station of maximum application for each function. Figures 9 and 10 show the result of insufficient strength in the rear most shaping function. The forebody is well contoured and the overall body plus wake is quite streamlined. The physical body, however, is rather blunt toward the stern end. The maximum diameter is about 12% larger than necessary and the drag is about 50% larger than it could be. By increasing the relative strength of the shaping function positioned with its maximum effect at the rear end of the physical body, the body shown in Figures 11 and 12 is obtained. The forebody shape is about the same as before but the maximum diameter has been reduced to 1% larger than the maximum constraint body diameter and the aft end is now trimmer. While the body may still appear to be somewhat blunt, the computed pressure drag coefficient of 0.00031 compared with an overall C_D of 0.00254* indicates that any

---

*Drag coefficient is based on an arbitrary reference area which is used for all computations. The changes in C_D therefore indicate the changes in actual drag resulting from body shape modifications. Ref. 12 gives 0.0010 as the C_D for an airship hull when normalized in this fashion. This value represents the limit to which the present calculation should proceed if the circumscribing body is positioned such that a smoothly tapering tail of minimum length can be produced. For comparison purposes, note that the surface area of a 6-to-1 prolate spheroid with major axis equal to 12 is 59.94. (The final body has a calculated

additional body shape modifications can at best result in a 10% reduction in drag** and that these modifications must be confined the last two sets of panels. To effect this change, the relative importance of the shape function which has its maximum influence in this region must be increased significantly. In retrospect, it appears that positioning the constraint body further forward in the circumscribing body would have provided additional panel sets for the optimizer to operate upon and would have yielded a more streamlined afterbody shape.

As the program now exists it can modify the circumscribing body only in the Y and Z directions. The length in the streamwise direction is fixed. Thus, in using the program one should take care to locate the upstream and downstream ends of the circumscribing body at those locations which experience indicates will yield a reasonable final shape. The program will then modify the Y and Z dimensions to produce the minimum drag possible for these locations consistent with constraint body dimensions.

It will be recognized that in this program we have attempted to model an inherently viscous flow phenomenon through the device of rep-representing the separated viscous wake behind the body by a pseudo-surface. This then permits one to obtain results agreeing reasonably well with reality from an inviscid flow analysis. The reason one must resort to such tricks is that the analysis of a fully viscous flow about a body is a problem perhaps two orders of magnitude more difficult than that of an inviscid flow about the same body. The strategem is not without pitfalls, however. Additional information of the type which would naturally be developed during the solution of the viscous flow problem must be supplied a priori to locate the wake attachment point and the downstream "stagnation" point. Since this kind of information is developed but slowly through the experimental correlations,

---

surface area of 58.37.) A 3-to-1 prolate spheroid with major axis equal to 6 has a surface area equal to 30.89. Replacing the aft half of a 3-to-1 ellipsoid by a right circular cone 9 units long yields a body with a surface area of 45.25. Assuming that the frictional drag is directly proportional to the surface area and that the remaining pressure drag can be eliminated through the use of a conical tail, the limiting C_D for the procedure becomes 0.00167. A further reduction would be possible if the tail could be shortened without inducing a pressure drag.

**The skin friction cannot be significantly reduced because the overall body length remains fixed and the minimum diameter is limited by a constraint body.

one must proceed cautiously. Nevertheless, the evidence to date indicates that astute modeling combined with optimal control techniques can result in a superior, cost-effective vehicle design technique.

Organizations wishing to experiment with the code in its present form can obtain copies through the contract monitor. Because computer core is much less expensive at NCSU than frequent disc read-writes, the program is configured to take advantage of all the core that could be conveniently assigned to one job (about 6,000 K-Bytes on an IBM 3081). This allocation permits one to provide about 196 panels on the physical body plus 28 for the wake body. Execution time is about 8 minutes per iteration. In principle, when larger computer memories and higher speed processors become available, bodies of greater complexity can be treated merely by increasing the array sizes and the appropriate DO loop limits.

The authors will endeavor to answer the questions of potential users of the code. A detailed user's manual is being prepared and will be available separately. This will include sample inputs, variable identification, and sample outputs.

Recommendation for Future Work

A computer code of this magnitude is necessarily evolutionary. Some potential additions which the authors feel should be investigated for possible inclusion are:

1. The panel normal velocity specification provision to permit the treatment of cooling flows. This is a relatively simple step, having been included in previous versions of the flow analysis code. It has been intended that this be done during the current grant period. Data sets for an actual light-twin engine nacelle and a possible redesign were prepared for use when this feature became available. Unexpected delays, principally those due to providing variable wake-body sizes and attachments, used the time allotted for this purpose, however.

2. The provision for treating propeller slipstreams. The previously-used package which computes only the axial flow component can be added relatively simply but the authors feel that replacing this with a computation employing trailing helical vortices, which can include the effect of wings protruding large distances from the body, should be strongly considered.

3. More rigorous separation criteria based on the velocity distributions in the local boundary layers for both laminar and turbulent flow. This would replace the rather arbitrary separation criterion now used which is based solely on the external pressure gradient.

4. A provision for accommodating small angles of attack. The original XYZ potential flow program included a provision for adding the effects of onset flows in the Y and Z directions. The streamline computation can also accommodate these cross flows. If one assumes that the boundary layer is thin enough that all of it moves in the same direction as the external flow, then the existing boundary layer computation method, modified in some fashion to account for the more rapid spreading of the streamlines associated with cross flows when compared with the axial flow over thin bodies and the more rapid curvature changes in the cross flow direction may possibly yield results which are adequate for design purposes if the velocity distribution in the neighborhood of the separation point can, at the same time, be determined more precisely. A complete finite-difference computation is not desired because of the computational time required. However, it may prove desirable to begin a two-dimensional finite difference computation at the point along each streamline where the pressure gradient becomes adverse.

5. A provision for including an axial scaling of the circumscribing body within the optimization procedure. Possibly this could take the form of two additional design variables, one applied to front half of the body and the other to the rear half.

The authors also feel that the user community would profit from additional exercise of the code. It would be possible thereby to acquire a better understanding of the effect of input parameter changes, location of the constraint body within the circumscribing body, and size relationship between the constraint body and the circumscribing body. They would be pleased to work with organizations endeavoring to undertake this activity.

References

1. Anderson, S. B., "General Overview of Drag," in Proceedings of the NASA • Industry • University General Aviation Drag Reduction Workshop, Published by Space Technology Center, University of Kansas, Lawrence, KS, 1975.

2. Vanderplaats, G. N., "CONMIN - A Fortran Program for Constrained Function Minimization," NASA TM X-62,282, 1973.

3. Vanderplaats, G. N., Hicks, Raymond N., and Murman, Earll M., "Application of Numerical Optimization Techniques to Airfoil Design," pp. 749-768, in Proceedings of Conference on Aerocynamic Analyses Requiring Advanced Computers, NASA SP-347, 1975.

4. Zoutendijk, G. G., Method of Feasible Directions, Elsevier, Amsterdam, 1960.

5. Vanderplaats, G. N. and Moses, Fred, "Structural Optimization by Method of Feasible Directions," Journal of Computers and Structures, Vol. 3, 1973, pp. 739-755.

6. Hess, J. L. and Smith, A. M. O., "Calculation of Non-Lifting Potential Flow About Arbitrary Three-Dimensional Bodies," Douglas Aircraft Company Report E.S. 40622, March 1962.

7. Dawson, Charles W. and Dean, Janet S., "The XYZ Potential Flow Program," Naval Ship Research and Development Center, Bethesda, MD, Report 3892, June 1972.

8. Smetana, F. O., Summey, D. C., Smith, N. S. and Carden, R. K., "Light Aircraft Lift, Drag, and Moment Prediction - A Review and Analysis," NASA CR 2523, May 1975.

9. Fox, S. R. and Smetana, F. O., "A Study of Cowl Shapes and Flow Port Locations for Minimum Drag and Effective Engine Cooling," NASA CR 159379, 117 pp. and NASA CR-159-380, 200 pp., November 1980.

10. Fox, S. R. and Smetana, F. O., "Integration of Propeller Slip-treams streams into the Aerodynamic Analysis of Bodies," SAE Business Aircraft Conference, April 1981, Paper No. 810566.

11. Haney, H. P. and Johnson, R. R., "Applications of Numerical Optimization to the Design of Wings with Specified Pressure Distributions," NASA CR-3238, February 1980.

12. Rouse, H., Elementary Mechanics of Fluids, New York: John Wiley and Sons, 1946, 376 pp.

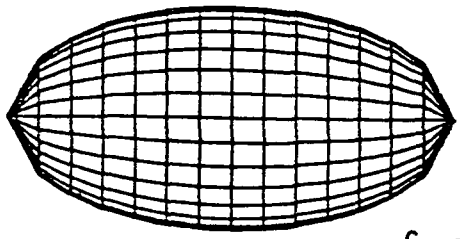

Figure 1. Circumscribing Ellipsoid

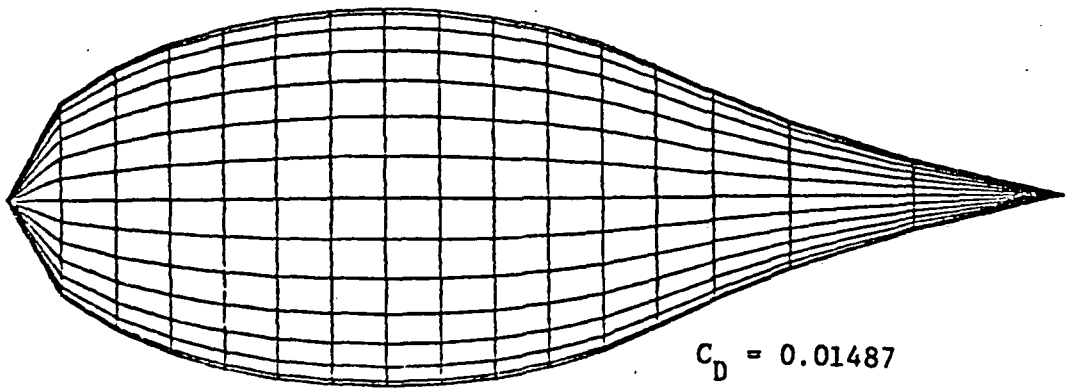

Figure 2. Ellipsoid with Wake Body
(Enlarged)

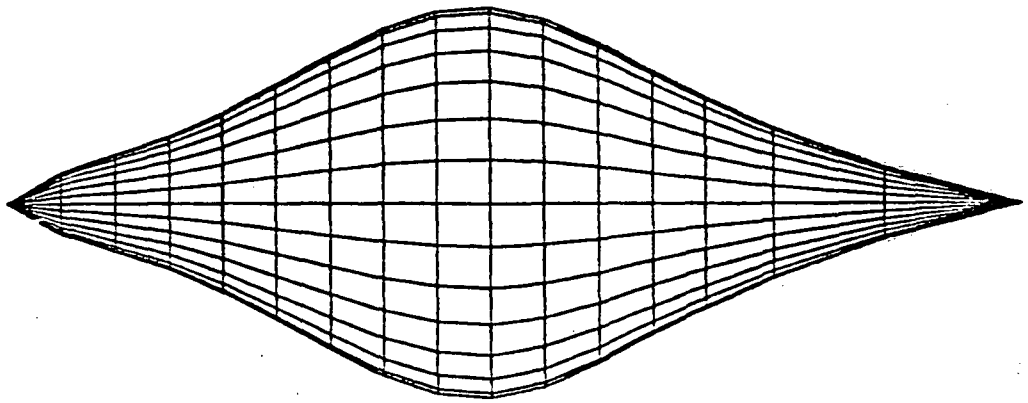

Figure 3. Ellipsoid with Contracted Bow and Stern

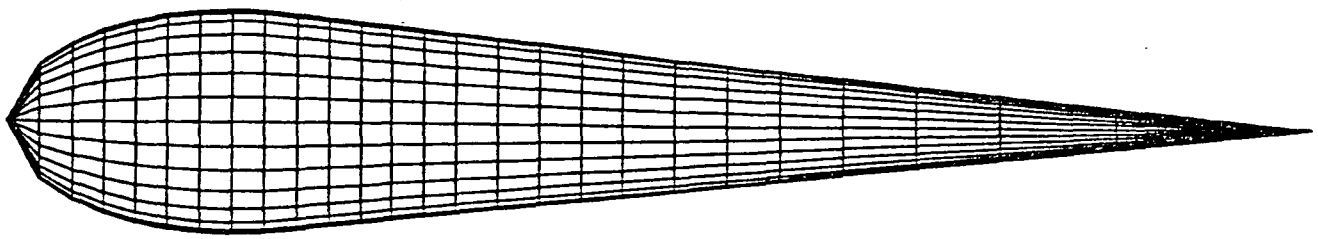

Figure 4. Ellipsoid with Extended Wake Body

Figure 5. Shrunk Body

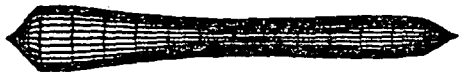

Figure 6. Body with Violated Constraints

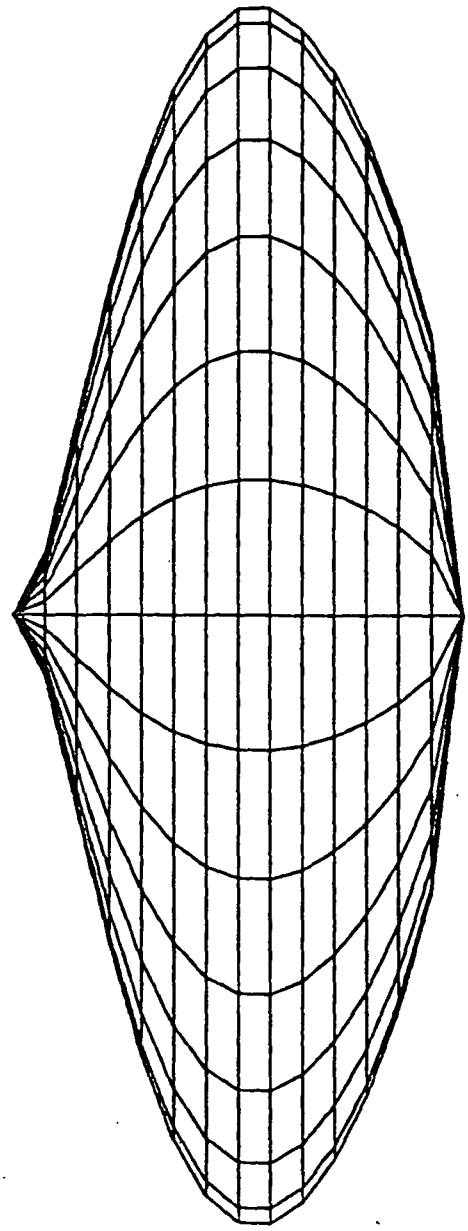

Figure 7. Unrealistic Body

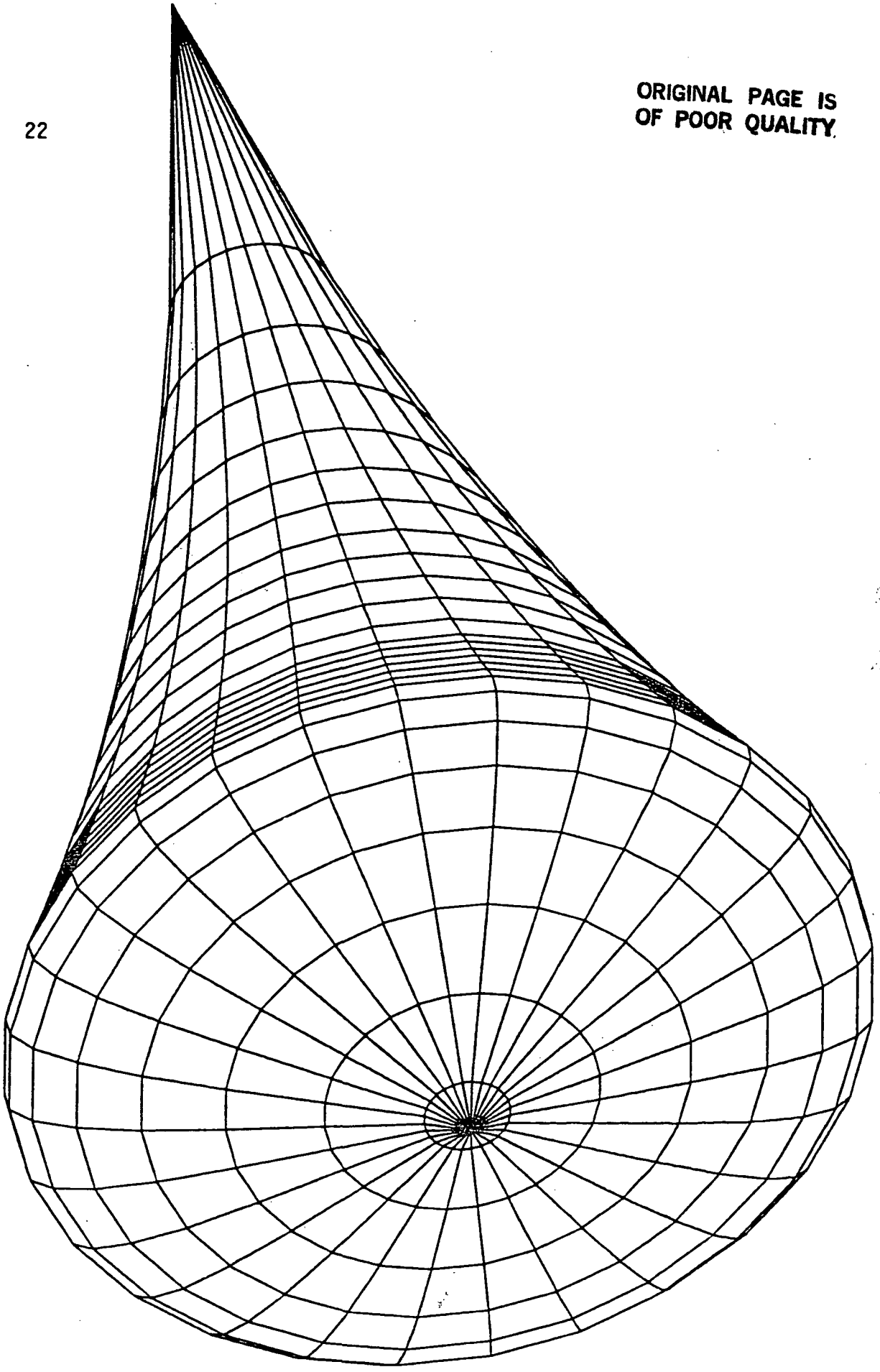

Figure 8. Unrealistic Body with Wake

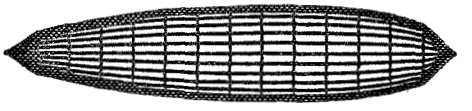

Figure 9. Intermediate Body Shape

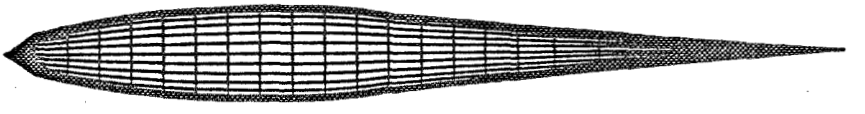

Figure 10. Intermediate Body Shape with Wake Body

$C_D = .00254$

Figure 11. New Body with Minimum Drag

Figure 12. New Body and Wake with Minimum Drag

1. Report No.	2. Government Accession No.	3. Recipient's Catalog No.
NASA CR-165984		

4. Title and Subtitle	5. Report Date
AUTOMATED DESIGN OF MINIMUM DRAG LIGHT AIRCRAFT FUSELAGES AND NACELLES	September 1982
	6. Performing Organization Code
7. Author(s)	8. Performing Organization Report No.
Frederick O. Smetana, Stan R. Fox, Baruch E. Karlin	
	10. Work Unit No.
9. Performing Organization Name and Address	
North Carolina State University Department of Mechanical & Aerospace Engineering Raleigh, NC 27607	11. Contract or Grant No. NSG-1584
	13. Type of Report and Period Covered
12. Sponsoring Agency Name and Address	Contractor report
National Aeronautics and Space Administration Washington, DC 20546	14. Sponsoring Agency Code 505-41-13-07

15. Supplementary Notes
Langley Technical Monitor: Scott O. Kjelgaard
Final Report

16. Abstract

The constrained minimization algorithm of Vanderplaats is applied to the problem of designing minimum drag faired bodies such as fuselages and nacelles. Body drag is computed by a variation of the Hess-Smith code. This variation includes a boundary layer computation. The encased payload provides arbitrary geometric constraints--specified a priori by the designer--below which the fairing cannot shrink. The optimization may include engine cooling air flows entering and exhausting through specific port locations on the body.

17. Key Words (Suggested by Author(s))	18. Distribution Statement
aircraft design drag minimization aircraft body flows	Unclassified-Unlimited Subject Category 02

19. Security Classif. (of this report)	20. Security Classif. (of this page)	21. No. of Pages	22. Price
Unclassified	Unclassified	25	A02